ELSEVIER

Journal of Nuclear Materials 275 (1999) 1–11

journal of nuclear materials

www.elsevier.nl/locate/jnucmat

Selection of materials as diluents for burning of plutonium fuels in nuclear reactors

H. Kleykamp

Forschungszentrum Karlsruhe, Institut für Materialforschung I, Postfach 3640, 76021 Karlsruhe, Germany

Received 5 October 1998; accepted 15 June 1999

Abstract

The relevant physical properties and the chemical behaviour of homogeneous and heterogeneous diluents in PuO_2 and PuN fissile materials are compiled and critically assessed. The out-of-pile properties of Al_2O_3, MgO, $MgAl_2O_4$, CeO_2, Ce_2O_3, Y_2O_3, ZrO_2, $CePO_4$, $ZrSiO_4$, B_4C, SiC, AlN, Mg_3N_2, Si_3N_4, CeN, YN and ZrN include, e.g. melting point, vapour pressure and thermal conductivity; the chemical behaviour towards steel, liquid sodium, water, air and nitric acid is reported. Promising diluents are AlN and ZrN, for which the dissolution behaviour in nitric acid was quantitatively examined. © 1999 Elsevier Science B.V. All rights reserved.

1. Introduction

Burning of fissile actinides in nuclear reactors requires inactive materials which act as diluents in the austenitic steel or Zircaloy clad fuel pins in order to soften the high fission density and consequently, the high fuel temperatures. One concept of actinide burning is the uranium free transmutation of long-lived isotopes that avoids the use of uranium in any chemical state and therefore, excludes continuous uranium–plutonium conversion during the irradiation process. Homogeneous and heterogeneous diluents are considered which form a solid solution with the fuel and a two-phase microstructure, respectively.

The compilation and the critical assessment cover the relevant physical properties and the chemical behaviour of different materials foreseen as homogeneous and heterogeneous diluents in uranium free PuO_2 and PuN fuels for the actinide transmutation programme [1–3]. The phase equilibria of the solid solutions and the two-phase materials of these pseudo-binary plutonium compound–diluent systems are described in the respective phase diagram manuals. In the case of a two-phase microstructure, the dispersed phase should be ideally the plutonium containing phase with 5–50 μm grain size. The compilation is focused on out-of-pile properties of the diluents. The irradiation behaviour is left out of consideration, e.g., activation, swelling or disintegration of the materials. The selection and the use of diluents are based on particular physical and chemical key properties which determine the preparation potential, handling, thermal stability during irradiation, reactions of defective pins with the coolant and the dissolution behaviour in acids during reprocessing. Some diluents were proposed before the knowledge of their unfavourable properties became available. The data compiled in Section 2 and in the Appendix A show that these diluents should be eliminated.

Diluents must have high melting points; other first order transition points must not appear or should occur at high temperatures only. Low vapour pressures and high thermal conductivities are required which should be lower and higher, respectively, than those of the fuels. A good compatibility with the cladding and with the coolant must be ensured, the material should be dissolvable in nitric acid. Fuels and heterogeneous diluents have to be compatible, i.e., thermodynamic equilibrium must exist, and in the case of eutectic systems, the eutectic temperatures must be high enough that liquefaction is avoided during the irradiation process. Fuels and heterogeneous diluents should hold similar total vapour pressures at given temperature. Otherwise, a redistribution and demixing could occur in the radial temperature gradient of a fuel pin during irradiation resulting in the recondensation of the phase with the highest vapour pressure in the coldest pin region. A major problem is

0022-3115/99/$ - see front matter © 1999 Elsevier Science B.V. All rights reserved.
PII: S 0 0 2 2 - 3 1 1 5 (9 9) 0 0 1 4 4 - 0

the assessment of the thermal conductivity of single-phase and two-phase materials which is a sensitive key property to structure and porosity. The following formula is recommended for the thermal conductivity λ of two-phase materials where the dispersed phase d is embedded in the continuous matrix phase m (λ_d and λ_m are the respective thermal conductivities and V_d is the volume fraction of the dispersed spherical phase) [4]

$$1 - V_d = (\lambda_d - \lambda)(\lambda_d - \lambda_m)^{-1}(\lambda_m/\lambda)^{1/3}. \tag{1}$$

The formula can be applied up to about 30 vol% of the dispersed phase. If the microstructure of the two-phase materials is unknown, especially in the case of equal volumes of both phases, the thermal conductivity should be estimated using the arithmetical mean of the thermal conductivities of the boundary phases. The formula for the thermal conductivity of two-phase materials can be applied also for porosity corrections in single-phase materials. If V_d is understood as the closed spherical porosity $P(0 \leqslant P < 1)$ and λ_d of the pores is set to zero, then Eq. (1) results in

$$\lambda = \lambda_m(1 - P)^{3/2}, \tag{2}$$

where λ_m is the thermal conductivity of the 100% dense material [4]. The thermal conductivity values of the fuels and diluents given in the following tables and in Appendix A are to 100% theoretical density (th.d.) corrected values using Eq. (2) where information on the density of the specimens is available.

2. Pre-selection of diluents

Selected properties of oxides, carbides and nitrides considered as homogeneous or heterogeneous diluents are compiled in the respective tables of Appendix A. These materials have adequate out-of-pile properties with the exception of B_4C, SiC, $ZrSiO_4$, $CePO_4$ and BN where specific features rule out the use as diluents.

- The carbides B_4C and SiC are of low thermodynamic stability though they have high melting points. The following Gibbs energies of formation at 727°C are reported [5]: $\Delta_f G°\langle B_4C\rangle = -61$ kJ/mol, $\Delta_f G°\langle SiC\rangle = -64$ kJ/mol, $4\Delta_f G°\langle Fe_2B\rangle = -272$ kJ/mol, $\Delta_f G°\langle FeSi\rangle = -76$ kJ/mol. In contrast with the Gibbs energies of formation of these phases are those of the high-stability transition metal carbides, e.g. $\Delta_f G°\langle ZrC\rangle = -188$ kJ/mol [5]. Therefore, the pseudo-binary systems B_4C–steel, SiC–steel and SiC–Zircaloy are not in thermodynamic equilibrium. The following reactions, e.g. with iron and zirconium are possible:

  $$B_4C + 8Fe \rightarrow 4Fe_2B + C \tag{3}$$

  (cf. [6,7])

  $$SiC + Fe \rightarrow FeSi + C \tag{4}$$

  (cf. [8,9])

  $$SiC + 2Zr \rightarrow ZrSi + ZrC \tag{5}$$

  (cf. [10, 11]).

  Out-of-pile compatibility studies evidence strong reactions starting at about 700°C. This temperature can be passed over in the respective PuO_2–B_4C, PuN–B_4C, PuO_2–SiC and PuN–SiC mixtures adjacent to the steel and Zircaloy claddings (hot spots).
- The phase $ZrSiO_4$ decomposes into ZrO_2 and SiO_2 at 1676°C, it is formed eutectoidally at this temperature [12].
- The phase $CePO_4$ has a very low thermal conductivity λ that increases unduly the pin centre temperature [13].
- The phase ^{11}BN has been also proposed as a heterogeneous diluent. Though the chemical behaviour is tolerable, the vapour pressure is adverse: total vapour pressure at 2000°C: 5×10^{-3} bar, no congruent melting point, the phase decomposes at about 2300°C [5]. However, the thermal conductivity is favourable: $\lambda = 29$ W/K m at 1000°C; $\lambda = 23$ W/K m at 1500°C; $\lambda = 21$ W/K m at 2000°C [14].

3. Properties of PuO_2 fuels and their diluents

Selected properties of PuO_2 and $PuO_{1.62}$ (oxygen poor phase boundary of the fcc homogeneity range of PuO_2 above 690°C) are compiled in Table 1. Problems of the chemical behaviour can arise with metals, liquid sodium and nitric acid. The compatibility of PuO_2 with steel claddings is ensured at least up to 600°C. If austenitic steels are considered as heterogeneous diluents, it is pointed out that the AISI 316 steel–PuO_2 system is a degenerate eutectic one with a eutectic temperature $T_e \approx 1433$°C. Metals with a high affinity to oxygen (e.g. chromium) reduce PuO_2 into the hypostoichiometric region of the homogeneity range which is linked with metal oxide (chromium oxide) formation above 1000°C. These results were deduced from the behaviour in the AISI 316 steel–UO_2 system [15]. PuO_2 reacts readily with sodium by the formation of $Na_4Pu_2O_5$. However, $PuO_{1.62}$ is compatible with sodium [16]. PuO_2 is not dissolvable in nitric acid without catalysts [17].

If the two preconditions, compatibility of PuO_2 with sodium and high-rate dissolution of PuO_2 in nitric acid, have to be strictly fulfilled, this type of fuel would not at all be qualified for transmutation experiments in sodium cooled fast reactors. In the case of disregard for these preconditions, the heterogeneous and homogeneous diluents Al_2O_3, MgO and $MgAl_2O_4$ as well as Ce_2O_3, Y_2O_3 and stabilised ZrO_2 (the latter one with

Table 1
Selected properties of PuO_2 and $PuO_{1.62}$ relevant to the uranium free actinide transmutation programme

Property	PuO_2	$PuO_{1.62}$
Melting point	2428°C [18]	2200°C [19]
Total vapour pressure at		
1500°C	4×10^{-10} bar [20]	$\simeq10^{-6}$ bar [20,25]
2000°C	3×10^{-7} bar [20]	$\simeq10^{-4}$ bar [20,25]
Thermal conductivity at		
1000°C	3.0 W/K m [21]	
1500°C	2.6 W/K m [21]	
2000°C	2.7 W/K m [21]	
Chem. behaviour towards		
Austenitic steel	No reaction below 1000°C [22–24]	No reaction below 1000°C [22–24]
Liquid sodium	Incompatible ($Na_4Pu_2O_5$ formation) [16]	No reaction [16]
Water	Oxide hydrate formation [26]	
Nitric acid, 110°C	Not dissolvable [17]	

restrictions) should be considered. The relevant out-of-pile properties and the chemical behaviour of these diluents and the constitution of the pseudo-binary diluent–PuO_2 systems are compiled in Appendix A.

4. Properties of PuN fuels and their diluents

PuN is a line compound and has a small homogeneity range on the plutonium rich side above 2000°C. It decomposes under 1 bar nitrogen at 2570°C into nitrogen saturated liquid plutonium and nitrogen, under 0.01 bar nitrogen already at 2300°C. No congruent melting was observed up to 25 bar nitrogen. Higher plutonium nitrides do not exist. The nitrogen partial pressure of PuN is only slightly higher than that of UN, whereas the plutonium partial pressure is markedly higher than the uranium partial pressure above UN. Liquid plutonium is formed above 1500°C due to the incongruent evaporation of PuN (low accommodation coefficient). The thermal conductivity of PuN is high, but about 50% lower than that of UN. PuN is compatible with austenitic steels up to 600°C and above and with sodium up to 890°C (boiling point of Na). The compound is dissolvable in HNO_3 and more slowly in HCl. Some results exist on the high rates of dissolution in different inorganic acids. The most important properties of PuN [27] and for comparison of UN [28] are compiled in Table 2.

Numerous heterogeneous metallic and ceramic diluents as well as homogeneous diluents were proposed for the PuN fuel. Table 3 reviews the phase behaviour of suitable PuN–M systems with M = V, Cr, Mo, W, Fe, Ni. The eutectic temperatures are decisive parameters for the selection of the diluent. In order to keep the ^{14}C production as low as possible during irradiation, the use of ceramic non-nitride diluents was proposed, e.g. $^{11}B_4C$

Table 2
Comparison of selected properties of UN with PuN relevant to the uranium free actinide transmutation programme [27,28]

Property	UN	PuN
Decomposition temperature under 1 bar N_2	2780°C [29,35]	2570°C [37]
Congruent melting point under 3 bar N_2	2830°C [30]	Incongruent [38]
Nitrogen partial pressure at		
1500°C	5×10^{-9} bar [31]	2×10^{-7} bar [39]
2000°C	3×10^{-5} bar [31]	1×10^{-4} bar [39]
Metal partial pressure at		
1500°C	5×10^{-10} bar [31]	1×10^{-6} bar [39]
2000°C	1×10^{-6} bar [31]	6×10^{-4} bar [39]
Thermal conductivity at		
1000°C	25 W/K m [32]	13 W/K m [40]
1500°C	27 W/K m [32]	14 W/K m [40]
2000°C	28 W/K m [32]	15 W/K m [40]
Chemical behaviour towards steels	No reaction below 600°C [33]	No reaction below 600°C [41]
Chemical behaviour towards liquid sodium	No reaction [34]	No reaction [41]
Reacts in boiling water to	U_3O_8 [28,36]	PuO_2 [41]
Dissolvable in concentrated acids, 110°C	In HNO_3 [28]	In HNO_3 and HCI [42]

Table 3
Selected properties of heterogeneous metallic diluents of PuN relevant to the uranium free actinide transmutation programme

System	Phase behaviour	Melting point of the metal [52]	Dissolution behaviour of the metal in concentrated nitric acid [53]
PuN–V	Eutectic, $T_e = 1270°C$, $x_{V,e} = 0.61$[a]	1910°C	Low rate of dissolution
PuN–Cr	Eutectic, $T_e = 1270°C$, $x_{Cr,e} = 0.62$[a]	1907°C	Cr passivates
PuN–Mo	Eutectic, $T_e = 2400°C$[b] [49]	2623°C	High rate of dissolution
PuN–W	Eutectic, $T_e = 2700°C$[b] [49]	3422°C	High rate of dissolution
PuN–Fe	Eutectic, $T_e = 1430°C$[b] [50]	1538°C	Fe passivates
PuN–Ni	Eutectic possible, see [51]	1455°C	Low rate of dissolution

[a] Calculated with the melting points and the enthalpies of melting of the phases.
[b] Eutectic temperatures of the corresponding UN–metal systems.

and SiC. However, the risk of hot-spot formation in these PuN–carbide mixtures adjacent to the steel cladding is high; therefore, the use of these carbides should be disregarded as explained in Section 2. TiN is not recommended as a heterogeneous diluent for PuN because of the limited solubility of about 3 mol% TiN in PuN at 2000°C (the data were derived from the corresponding UN–TiN system [43]). The use of CrN cannot be supported as Cr nitrides have high nitrogen partial pressures, e.g. $p(N_2) = 1$ bar for CrN at 1048°C [44]. Further, the use of VN and NbN is questionable because – in the pseudo-binary UN–(V, Nb)N systems–ternary nitrides are formed. The existence of ternary nitrides in the PuN–(V, Nb)N systems has not yet been proved [45]. The application of Mg_3N_2 as heterogeneous diluent has to be rejected due to its limited thermal stability [46]. The use of rare earth nitrides as homogeneous diluents should be rated in the light of the extreme difficulties of the preparation of oxygen poor nitrides [47,48]. The most promising candidates as heterogeneous and homogeneous diluents in PuN are AlN and ZrN, respectively. As the dissolution behaviour of these materials in nitric acid has not yet been investigated the recent experimental results are communicated in Section 5. The most important properties of the nitride diluents AlN, Mg_3N_2, Si_3N_4, CeN, YN and ZrN are compiled in Appendix A.

5. Dissolution experiments of AlN and ZrN in nitric acid

5.1. Materials

The AlN materials used for the dissolution experiments in nitric acid were supplied by two manufacturers in the form of dense sintered rods, which were cut into cubes: (1) Elektroschmelzwerk Kempten (ESK), Kempten, Germany. Impurities: oxygen: 3%; carbon: 0.06%; other metallic impurities: <0.5%; density: 94% th.d. (2) Tokuyama Soda, Tokyo, Japan. Impurities: oxygen: 0.3 %; carbon: 0.03 %; other metallic impurities:<0.2%; density: 93% th.d.

ZrN powder was supplied by the company H.C. Starck, Goslar, Germany. Impurities: ≈0.1%; zirconium: 87.6%; nitrogen: 12.3%; corresponding to the composition $ZrN_{0.91}$. The powder was hot-pressed in the form of cylindrical pellets at two different temperatures which resulted in two geometric densities of 82% and 89% th.d., respectively.

Nitric acid p. a. in excess was used for the dissolution experiments with mass ratios HNO_3/solids of about 200. This high mass ratio is necessary to avoid an influence of a high-concentrated solution on the dissolution kinetics, e.g., an increase of the formal reaction order in the progress of the dissolution process.

5.2. Results

5.2.1. AlN

The measured and weighed cubes with initial masses typically of 0.25 g were incompletely dissolved in 7 M HNO_3 at boiling temperature (110°C) up to 21 h and were weighed again. Each dissolution experiment was started with fresh material. Only about 1% of the ESK material was dissolved after 21 h. The kinetics followed a parabolic time law after an incubation period up to 2 h. With the mass decrease $m_0 - m = \Delta m$ and the initial geometric surface F_0, the time law

$$(\Delta m/F_0)^2 = kt \tag{6}$$

and the rate constant of dissolution $k = 0.125$ mg^2/cm^4 h were obtained. The Tokuyama Soda material was nearly completely dissolved after 15 h. This kinetics could be approximated by a linear time law after an incubation period up to 3 h which gives

$$\Delta m/F_0 = kt, \tag{7}$$

with $k = 18$ mg/cm^2 h. The dissolution results of both materials are graphically presented in Fig. 1 in the form of log $(\Delta m/F_0)$ as a function of the dissolution time.

A high-dense white layer was observed on the surface of partly dissolved Tokuyama Soda material. X-ray microanalysis of this layer indicated AlN with

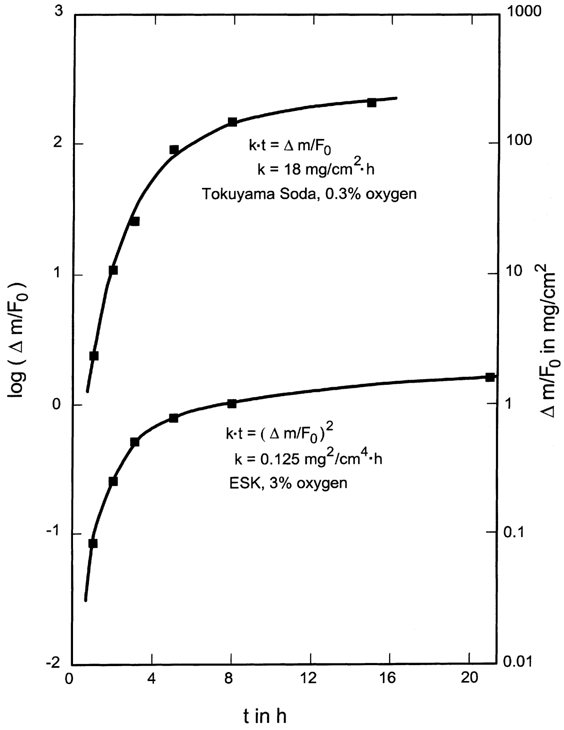

Fig. 1. Dissolution rate of two AlN materials (Tokuyama Soda and Elektroschmelzwerk Kempten) in 7 M HNO_3 at 110°C as a function of time.

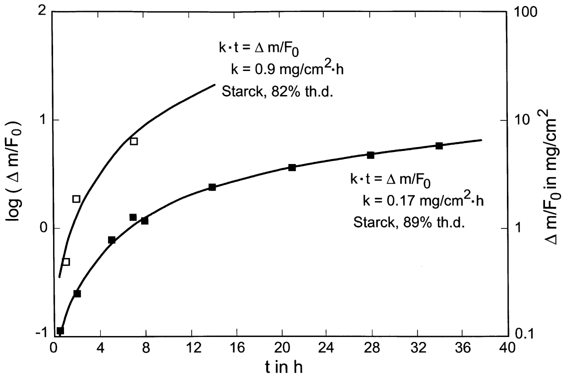

Fig. 2. Dissolution rate of ZrN (Dr. H.C. Starck) of two sintering densities in 7 M HNO_3 at 110°C as a function of time.

small amounts of oxygen and carbon; X-ray diffraction resulted in hexagonal AlN with the lattice parameters $a = 310.9$ pm and $c = 497.7$ pm. The reason for the large difference of the dissolution behaviour of the two types of AlN is the high oxygen content of the ESK material which had formed Al_2O_3 layers on the AlN grain surfaces during the fabrication process. Pure Al_2O_3 is not dissolvable in HNO_3. The rate determining step of the dissolution process of AlN is a grain boundary diffusion controlled one in the Al_2O_3 layers. On the other hand, the oxygen content in the Tokuyama Soda material is low and is probably below the oxygen solubility in AlN. Therefore, the concentration of this impurity seems not to influence the dissolution behaviour of AlN.

5.2.2. ZrN

The measured and weighed cylindrical slabs with initial masses between 0.3 and 0.6 g and sintering densities of 82% and 89% th.d. were incompletely dissolved under the same conditions as AlN up to 34 h. Only about 1.5% of the material with the higher density was dissolved after this period. The kinetics could be approximated by a linear time law given in Eq. (7) with the rate constant of dissolution $k = 0.17$ mg/cm^2 h for ZrN with 89% th.d. and $k = 0.9$ mg/cm^2 h for the material with the lower sintering density of 82% th.d. The dissolution results of ZrN with two different sintering densities are graphically presented in Fig. 2 in the form of log ($\Delta m/F_0$) as a function of the dissolution time.

The dissolution process is subject to the rate laws of the heterogeneous kinetics and is characterised in the isothermal mode by a dissolution rate constant k which indicates the mass loss $m_0 - m = \Delta m$ per unit area F_0 and time t. The rate of the mass decrease of an unprotected solid is only proportional to the contact area with the solvent. Therefore, the dissolution process can be described formally by a zero-order reaction

$$\mathrm{d}m/\mathrm{d}t = -kF_0. \tag{8}$$

Other influences, e.g., porosity and sinter density of a solid, are included in the rate constant of dissolution k. In the case of ZrN, the low-density material has a higher open porosity and a higher contact area with the solvent, respectively, than 100% dense material and consequently a larger dissolution rate constant. In conclusion, oxygen poor AlN (93% th.d.) is easily dissolvable in 7M HNO_3 with $k = 18$ mg/cm^2 h; whereas ZrN (89% th.d.) is more heavily dissolvable with $k = 0.17$ mg/cm^2 h. However, the porosity, i.e. the inner surface has a high influence on the rate of dissolution. For comparison with AlN and ZrN, the following k values are given for other materials dissolved under the same conditions: molybdenum, $k = 1030$ mg/cm^2 h; UO_2, $k = 100$ mg/cm^2 h; palladium, $k = 0.5$ mg/cm^2 h; PuO_2, $k = 10^{-5}$ mg/cm^2 h [54].

6. Conclusions

Homogeneous diluents reduce in general the thermal conductivity of the fuel phase. On the other hand, heterogeneous diluents according to the level of their thermal conductivity can increase the thermal conductivity of the two-phase material. Molybdenum and tungsten as well as Al_2O_3, MgO, $MgAl_2O_4$ and with restrictions stabilised ZrO_2 are promising candidates. Moreover, heterogeneous diluents are available with total vapour pressures that are comparable to those of the fuels. Higher vapour pressures may result in redistribution effects during irradiation.

This study has demonstrated further the excellent physical properties of AlN and ZrN: high melting points, low vapour pressures, very high thermal conductivities; good chemical behaviour towards the steel cladding, sodium and nitric acid. Therefore, AlN and ZrN are recommended as heterogeneous and homogeneous diluents, respectively, in PuN fuel. ZrN can be considered also as diluent for PuO_2 fuel because these materials form a stable thermodynamic couple. Probably some oxygen can be dissolved in ZrN whereas PuO_2 is reduced into its hypostoichiometric region. The situation is not as clear for the PuO_2–AlN couple where the formation of PuN, Al_2O_3 and a third phase is possible. Compatibility tests are therefore necessary.

Appendix A. Physical properties and chemical behaviour of homogeneous and heterogeneous diluents

(1) **Al_2O_3**

Melting point	2054°C	[55]
Total vapour pressure at 1950°C	≈10^{-6} bar	[53]
Thermal conductivity at		
500°C	13.3 W/K m	[59]
1000°C	8.2 W/K m	[59]
1500°C	5.8 W/K m	[59]
Chemical behaviour towards		
Iron	No reaction below 900°C	[55]
Liquid sodium	No reaction	[60,61]
Water	Bulk material not dissolvable	[53]
Nitric acid	Not dissolvable	[53]

The Al_2O_3–PuO_2 system is eutectic: $T_e = 1910°C$, $x_e = 58$ mol% Al_2O_3 [56–58]. The thermal conductivity of 25 vol.% PuO_2 in 75 vol.% Al_2O_3 was calculated with Eq. (1) which gives for 100% th.d. material: $\lambda = 6.6$ W/K m at 1000°C and $\lambda = 4.9$ W/K m at 1500°C. The Al_2O_3–$PuO_{1.62}$ system is eutectic: $T_e = 1776°C$, $x_e = 48$ mol% Al_2O_3 [57,58]. The lowest melting in the ternary Al_2O_3–MgO–PuO_2 system starts at 1860°C [57,58].

(2) **MgO**

Melting point	2827°C	[55]
Total vapour pressure at 1727°C	≈10^{-4} bar	[5,62]
Thermal conductivity at		
500°C	20 W/K m	[63]
1000°C	13 W/K m	[63]
1500°C	6 W/K m	[14]
2000°C	5 W/K m	[14]
Chemical behaviour towards		
Iron	No reaction below 1100°C	[64]
Liquid sodium	No reaction	[61,65]
Water	Hydroxide formation	[53]
Nitric acid	Low rate of dissolution	[53]

The MgO–PuO_2 system is eutectic: $T_e = 2260°C$, $x_e = 60$ mol% MgO; 3 mol% PuO_2 are soluble in MgO [56–58]. The thermal conductivity of 25 vol.% PuO_2 in 75 vol.% MgO was calculated with Eq. (1) which gives for 100% th.d. material: $\lambda = 9.8$ W/K m at 1000°C and 5.7 W/K m at 2000°C. The MgO–$PuO_{1.62}$ system is eutectic: $T_e = 2068°C$, $x_e \approx 50$ mol% MgO [57,58].

(3) **$MgAl_2O_4$**

Melting point	2105°C	[55]
Thermal conductivity at		
500°C	9.0 W/K m	[59]
1000°C	7.7 W/K m	[59]
1500°C	≈8 W/K m	[59]
Chemical behaviour towards liquid sodium	No reaction	[61]

(4) **CeO_2**

Melting point	≈2400°C	[66]
Total vapour pressure at		
1500°C	2×10^{-7} bar	[67]
2000°C	6×10^{-5} bar	[67]
Thermal conductivity at		
1000°C	1.2 W/K m	[14]
1500°C	0.9 W/K m	[14]
2000°C	1.2 W/K m	[14]
Chemical behaviour towards		
Austenitic steel	No reaction below 650°C	[68]
Liquid sodium	Incompatible ($NaCeO_2$ formation)	[68]
Water	Not dissolvable	[69]
Nitric acid	Low rate of dissolution	[70]

The CeO_2–PuO_2 system is completely miscible in the solid [71]. (Ce, Pu)O_2 is incompatible with sodium [72]. The congruent melting point of Ce_2O_3 is 2142°C [66]. The thermal conductivity of Ce_2O_3 (hexagonal) is not available. However, the following data were reported, e.g. at 1000°C, for Sm_2O_3 (monoclinic): $\lambda = 1.3$ W/K m; Er_2O_3 (cubic): $\lambda = 2.1$ W/K m; Lu_2O_3 (cubic): 2.2 W/K m [73]. There is an extended solid solubility in the Ce_2O_3–PuO_2 system up to 50 mol% $CeO_{1.5}$ in PuO_2. Ce_2O_3 and sodium are compatible [68]. A limited solid solubility of Ce_2O_3 exists in $PuO_{1.62}$. The (Ce, Pu)$_2O_3$ solid solution is compatible with sodium [72].

(5) **Y_2O_3**

Melting point	2430°C	[74]
Total vapour pressure at 2000°C	2×10^{-7} bar	[75]
Thermal conductivity at		
500°C	4.1 W/K m	[76]
1000°C	2.5 W/K m	[76]
1500°C	2.9 W/K m	[77]
2000°C	≈4 W/K m	[77]
Chemical behaviour towards		
Refractory metals	No reaction below 1500°C	[78]
Liquid sodium	No reaction	[60]
Water	Slowly dissolvable	[53]
Nitric acid	Low rate of dissolution	[53]

An extended solid solubility of Y_2O_3 exists in the Y_2O_3–PuO_2 system up to about 90 mol% $YO_{1.5}$ at 1500°C [79].

(6) **ZrO_2**

Melting point	2710°C	[74]
Total vapour pressure at 2000°C	10^{-8} bar	[80]
Thermal conductivity at		
1000°C	2.2 W/K m	[81]
1500°C	1.5 W/K m	[14]
2000°C	1.8 W/K m	[14]
Chemical behaviour towards		
Iron	No reaction below 1200°C	[82]
Liquid sodium	No reaction	[61]
Nitric acid	Not dissolvable	[53,83]

The ZrO_2–PuO_2 system is not completely miscible due to the tetragonal structure of ZrO_2 in the temperature range 1200–2300°C and the monoclinic structure below 1200°C [84]. The transitions can be suppressed by stabilisation of ZrO_2 with CaO or Y_2O_3. Complete miscibility of stabilised ZrO_2 with PuO_2 is expected. The ZrO_2–Y_2O_3 system forms an fcc solid solution above 15 wt% Y_2O_3 [85]. The thermal conductivity of ZrO_2–15 wt% Y_2O_3 is 1.6 W/K m at 500°C, 1.7 W/K m at 1000°C [76] and about 2 W/K m between room temperature and 1500°C [75].

(7) **$CePO_4$**

Melting point	2045°C	[86]
Thermal conductivity at		
500°C	1.8 W/K m	[13]
1000°C	≈1.7 W/K m	[87]
Chemical behaviour towards water	Not dissolvable	[87]

(8) **$ZrSiO_4$**

Melting point	None	[12]
Eutectoidal formation	1676°C	[12]
Thermal conductivity at		
500°C	5.4 W/K m	[88]
1000°C	4.5 W/K m	[88]
1500°C	4.2 W/K m	[88]

(9) **$^{11}B_4C$**

Homogeneity range	9–19 at.% C	[89]
Melting point	2450°C (≈18 at.% C)	[74]
Total vapour pressure at 2000°C	≈0.5 bar	[46]
Thermal conductivity at		
20°C	25 W/K m	[90]
1000°C	15 W/K m	[90]
1500°C	≈15 W/K m	[90]
Chemical behaviour towards		
Austenitic steel	No reaction below 700°C	[67,90,91]
Liquid sodium	No reaction	[61,92]
Water	Not dissolvable	[92]
Nitric acid	Not dissolvable	[92]
Air	Compatible below 500°C	[90]

The B_4C–austenitic steel system is thermodynamically unstable. (Fe, Cr)$_2$B occurs at about 700°C which forms a eutectic with austenitic steel at $T_e = 1226$°C [6,7,90].

(10) SiC

Melting point	2830°C (peritectic)	[93]
Stable modification	Hex. α-SiC	[93]
Silicon partial pressure at 2000°C	1.0×10^{-4} bar	[94]
Total vapour pressure at 2000°C	1.4×10^{-4} bar	[94]
Thermal conductivity of		
α-SiC at 1000°C	47 W/K m	[95]
α-SiC at 1500°C	31 W/K m	[95]
β-SiC at 1000°C	40 W/K m	[95]
β-SiC at 1500°C	30 W/K m	[95]
Chemical behaviour towards		
Austenitic steel	Compatible below 700°C	[8–11]
Liquid sodium	No reaction below 500°C	[96]
Water	Compatible	[53]
Nitric acid	Not dissolvable	[53]
Air	Compatible below 1500°C	[97]

The SiC–austenitic steel system is thermodynamically unstable. Silicides form at about 700°C. The lowest ternary eutectic in the Fe–Si–C system is located at 1200°C [8–11].

(11) AlN

Melting point	Incongruent	[98]
Nitrogen partial pressure at 2000°C	10^{-3} bar	[46]
Total vapour pressure at 2000°C	10^{-1} bar	[99]
Decomposes under 1 bar nitrogen	2417°C	[98]
Thermal conductivity at		
500°C	62 W/K m	[59]
1000°C	36 W/K m	[59]
1500°C	27 W/K m	[59]
Chemical behaviour towards		
Austenitic steel	Compatible below 1000°C	[100]
Boiling water	Slow hydrolysis	[101]
Liquid sodium	Probably compatible	[102]
Nitric acid, 110°C	High rate of dissolution, k = 18 mg/cm^2 h for 93% th.d.	[a]
Air	Up to 700°C no reaction	[102,103]

[a] This study

There is no mutual solid solubility in the AlN–PuN system.

(12) Mg_3N_2

Melting point	Incongruent	[74]
Nitrogen partial pressure at 1000°C	10^{-8} bar	[46]
Decomposes under 1 bar nitrogen	<1500°C	[74]
Chemical behaviour towards		
Water	Hydrolysis	[53]
Nitric acid	Dissolvable	[53]

(13) Si_3N_4

Melting point	Incongruent	[5]
Nitrogen partial pressure at 1500°C	5×10^{-3} bar	[104]
Decomposes under 1 bar nitrogen	1878°C	[5]
Thermal conductivity at		
500°C	12 W/K m	[105]
1000°C	9 W/K m	[105]
1500°C	10 W/K m	[105]
2000°C	12 W/K m	[105]
Chemical behaviour towards		
Austenitic steel	Compatible below 900°C	[106]
Iron	Compatible below 700°C	[107]
Liquid sodium	No reaction	[108]
Water	Not dissolvable	[53]
Nitric acid	Not dissolvable	[53]

(14) CeN

Melting point	2480°C	[74]
Nitrogen partial pressure at		
1500°C	4×10^{-8} bar	[46]
2000°C	4×10^{-4} bar	[46]
Thermal conductivity (800–2000°C)	5 W/K m	[109]

Chemical behaviour towards		
Water	Decomposes	[110]
Nitric acid	Dissolvable	[110,111]
Oxygen	Rapid oxidation at room temperature	[47]

The CeN–PuN system is completely miscible in the solid [112].

(15) **YN**

Melting point	2670°C (?), decomposes (?)	[74]
Nitrogen partial pressure at		
1500°C	$\approx 10^{-7}$ bar	[46]
2000°C	$\approx 10^{-3}$ bar	[46]
Chemical behaviour towards		
Nitric acid	Dissolvable	[110]
Oxygen	Rapid oxidation at room temperature	[48]

The YN–PuN system is completely miscible in the solid [112].

(16) **ZrN**

Homogeneity range	40–60 at.% N	[74]
Melting point	2960°C	[74]
Nitrogen partial pressure at		
1500°C	$\approx 10^{-12}$ bar	[46]
2000°C	$\approx 10^{-7}$ bar	[46]
Thermal conductivity at 500°C	17 W/K m	[113]
1000°C	23 W/K m	[113]
1500°C	26 W/K m	[113]
2000°C	24 W/K m	[113]
Chemical behaviour towards		
Austenitic steel	Formation of Zr_4M_2N possible	[114]
Water	Not dissolvable	[53]
Nitric acid, 110°C	Tolerable rate of dissolution, $k = 0.17$ mg/ cm^2 h for 89% th.d.	[b]
Air	No oxidation at room temperature	[53]

[b] This study.

The ZrN–PuN system is completely miscible in the solid [112].

References

[1] A. Languille, P. Millet, J. Rouault, S. Pillon, J. Alloys Compounds 271–273 (1998) 517.

[2] M. Burghartz, Hj. Matzke, C. Léger, G. Vambenepe, M. Rome, J. Alloys Compounds 271–273 (1998) 544.

[3] M. Beauvy, T. Duverneix, C. Berlanga, R. Mazoyer, C. Duriez, J. Alloys Compounds 271–273 (1998) 557.

[4] Schulz, High Temp. High Press. 13 (1981) 649.

[5] M.W. Chase, NIST-JANAF Thermochem. Tables, 4th ed., 1998.

[6] L.R. Bunnell, in: BNWL-1349-2, 1970, p. 6.1.

[7] D.E. Baker, R.E. Dahl, in: HEDL-TME-71-66, 1971, p. HEDL-118.

[8] K.M. Geib, C.W. Wilmsen, J.E. Mahan, M.C. Bost, J. Appl. Phys. 61 (1987) 5299.

[9] Y. Pan, J.L. Baptista, J. Am. Ceram. Soc. 79 (1996) 2017.

[10] L. Brewer, O. Krikorian, J. Electrochem. Soc. 103 (1956) 38.

[11] Yu.I. Krylov, V.A. Bronnikov, V.G. Krysina, V.V. Pristavko, Soviet Powder Metall. Met. Ceram. (1975) 1000.

[12] W.C. Butterman, W.R. Foster, Am. Mineralogist 52 (1967) 884.

[13] Y. Hikichi, T. Nomura, Y. Tanimura, S. Suzuki, M. Miyamoto, J. Am. Ceram. Soc. 73 (1990) 3594.

[14] C.D. Pears, ASD-TDR-62-765, 1963.

[15] H. Kleykamp, J. Nucl. Mater. 247 (1997) 103.

[16] S. Pillon, CEA-R-5489, 1989.

[17] D. Vollath, H. Wedemeyer, H. Elbel, E. Günther, Nucl. Technol. 71 (1985) 240.

[18] M.G. Adamson, E.A. Aitken, R.W. Caputi, J. Nucl. Mater. 130 (1985) 349.

[19] B. Riley, Sci. Ceram. 5 (1970) 83.

[20] W.M. Pardue, D.L. Keller, J. Am. Ceram. Soc. 47 (1964) 610.

[21] Y. Philipponneau, CEA Cadarache, unpublished report, 1990.

[22] M.B. Waldron, A.G. Adwick, H. Lloyd, M.J. Notley, D.M. Poole, L.E. Russell, J.B. Sayers, Proc. Second UN Geneva Conference 1958 6 (1959) 690.

[23] M. Zambernard, NUMEC-P-105 (1963) 33.

[24] D.F. Carroll, BNWL-18, 1965.

[25] R.J. Ackermann, R.L. Faircloth, M.H. Rand, J. Phys. Chem. 70 (1966) 3698.

[26] J.L. Stakebake, J. Nucl. Mater. 38 (1971) 241.

[27] H. Holleck, H. Kleykamp, in: Gmelin Handbook of Inorganic Chemistry, Transuranium Elements, Part C, Verlag Chemie, Weinheim, 1972, p. 83.

[28] H. Holleck, H. Kleykamp, in: Gmelin Handbook of Inorganic Chemistry, Uranium Suppl, Part C 7, Springer, Berlin, 1981, pp. 1–93.

[29] W.M. Olson, R.N.R. Mulford, J. Phys. Chem. 67 (1963) 952.

[30] R. Benz, W.B. Hutchinson, J. Nucl. Mater. 36 (1970) 135.

[31] K.A. Gingerich, J. Chem. Phys. 51 (1969) 4433.

[32] A.B.G. Washington, TRG-2236, 1973.

[33] O. Götzmann, F. Thümmler, in: Proceedings of the Sixth Plansee Seminar, Reutte /Tyrol, 1968, 1969, p. 439.

[34] M.G. Chasanov, P.A. Nelson, A.D. Tevebaugh, J. Nucl. Mater. 16 (1965) 227.

[35] J. Bugl, A.A. Bauer, J. Am. Ceram. Soc. 47 (1964) 425.
[36] J.J. Katz, G.T. Seaborg, The Chemistry of the Actinide Elements, McGraw-Hill, New York, 1957, p. 151.
[37] F.L. Oetting, Chem. Rev. 67 (1967) 261.
[38] W.M. Olson, R.N.R. Mulford, J. Phys. Chem. 68 (1964) 1048.
[39] C.A. Alexander, J.S. Ogden, W.M. Pardue, BMI-1862, 1969, p. A7.
[40] C.A. Alexander, R.B. Clark, O.L. Kruger, J.L. Robbins, in: H. Blank, R. Lindner (Eds.), Plutonium and other Actinides, North-Holland, Amsterdam, 1976, p. 277.
[41] W.M. Pardue, V.W. Storhok, R.A. Smith, in: A.E. Kay, M.B. Waldron (Eds.), Plutonium 1965, Chapman and Hall, London, 1967, p. 721.
[42] W.M. Pardue, V.W. Storhok, R.A. Smith, P.H. Bonnell, J.E. Gates, D.L. Keller, BMI-1693, 1964.
[43] H. Holleck, E. Smailos, F. Thümmler, Monatsh. Chem. 99 (1968) 985.
[44] J.D. Browne, P.R. Liddell, R. Street, T. Mills, Phys. Stat. Sol. (a) 1 (1970) 715.
[45] H. Holleck, KfK-3087 B, 1981.
[46] I. Barin, Thermochem. Data of Pure Substances, 3rd ed., Verlag Chemie, Weinheim, 1995.
[47] H. Holleck, E. Smailos, F. Thümmler, J. Nucl. Mater. 28 (1968) 105.
[48] H. Holleck, Proc. Thermod. Nucl. Mater., IAEA, Vienna, 1975, pp. 213.
[49] C. Politis, F. Thümmler, H. Wedemeyer, J. Nucl. Mater. 38 (1971) 132.
[50] G. Briggs, J.P. Guha, J. Barta, J. White, Trans. Brit. Ceram. Soc. 62 (1963) 221.
[51] J.P. Guha, J. Nucl. Mater. 45 (1972) 40.
[52] A.T. Dinsdale, NPL-DMA (A) 195 (1989).
[53] H. Remy, Lehrbuch der Anorganischen Chemie, 13th ed., Leipzig, 1970.
[54] H. Kleykamp, in: Proc. Jahrestagung Kerntechnik ’85, 1985, München, p. 329.
[55] G. Petzow, G. Effenberg, Ternary Alloys, Verlag Chemie, Weinheim, 1993, vol. 6, p. 460; vol. 5, p. 325.
[56] A. Hough, J.A.C. Marples, J. Nucl. Mater. 15 (1965) 298.
[57] H. Zhang, M.E. Huntelaar, R.J.M. Konings, E.H.P. Cordfunke, J. Nucl. Mater. 249 (1997) 223.
[58] H. Zhang, M.E. Huntelaar, R.J.M. Konings, E.H.P. Cordfunke, J. Nucl. Mater. 250 (1997) 83.
[59] M. Rohde, B. Schulz, ASTM-STP-1125 (1992) 764.
[60] F.L. Epstein, J. Nigriny, AECD-3709, 1948.
[61] J.K. Fink, J.J. Heiberger, R. Kumar, R. Blomquist, L. Leibowitz, E.S. Sowa, J.R. Pavlik, L. Baker, ANL-75-74, 1976.
[62] F. Born, Z. Elektrochem. 31 (1925) 309.
[63] F.R. Charvat, W.D. Kingery, J. Am. Ceram. Soc. 40 (1957) 306.
[64] P.M. Valet, W. Pluschkell, H.J. Engell, Arch. Eisenhw. 46 (1975) 383.
[65] R.W. Ditchburn, J. Harding, Nature 136 (1935) 70.
[66] O.A. Mordovin, N.I. Timofeeva, L.N. Drozdova, Inorg. Mater. USSR 3 (1967) 159.
[67] B.S. Kulvarskaya, R.S. Maslovskaya, Radio Eng. Electron. USSR 5 (1960) 89.
[68] M.A. Mignanelli, P.E. Potter, M.G. Barker, J. Nucl. Mater. 97 (1981) 213.
[69] N.I. Timofeeva, L.N. Drozdova, V.A. Timofeev, Inorg. Mater. USSR 6 (1970) 539.
[70] S.S. Moosath, K.N.N. Kurup, Chem. Ind. London, 1958, p. 1321.
[71] M.S. Farkas, BMI-X-10175, 1966.
[72] M.A. Mignanelli, P.E. Potter, J. Nucl. Mater. 125 (1984) 182.
[73] V.P. Zhuze, O.N. Novruzov, A.A. Popova, A.I. Shelykh, Inorg. Mater. USSR 4 (1968) 1304.
[74] T.B. Massalski, Binary Alloy Phase Diagrams, 2nd ed., ASM Int., 1990.
[75] L.N. Grossman, GEST-2022, 1964.
[76] E.S. Fitzsimmons, DC-61-6-4, 1961.
[77] A.D. Feith, GEMP-296, 1964.
[78] L.N. Grossman, CONF-650908-5, 1965.
[79] E.E. Jackson, M.H. Rand, AERE-R-3636, 1963.
[80] W.A. Chupka, J. Berkowitz, M.G. Inghram, J. Chem. Phys. 26 (1957) 1207.
[81] M. Adams, J. Am. Ceram. Soc. 37 (1954) 74.
[82] T. Katsura, M. Wakihara, S. Hara, T. Sugihara, J. Solid State Chem. 13 (1975) 107.
[83] G. Scagliarini, Atti Linc. [6] 4 (1926) 204.
[84] P.G. Mardon, D.J. Hodkin, J.T. Dalton, J. Nucl. Mater. 32 (1969) 126.
[85] V.S. Stubican, R.C. Hink, S.P. Ray, J. Am. Ceram. Soc. 61 (1978) 17.
[86] Y. Hikichi, T. Nomura, J. Am. Ceram. Soc. 70 (1987) C-252.
[87] K. Bakker, H. Hein, R.J.M. Konings, R.R. van der Laan, Hj. Matzke, P. van Vlaanderen, J. Nucl. Mater. 252 (1998) 228.
[88] F.H. Norton, W.D. Kingery, NYO-602, 1952.
[89] K.A. Schwetz, P. Karduck, J. Less-Common Met. 175 (1991) 1.
[90] S. Ihara, K. Tanaka, Mitsubishi Metal Corp., unpublished report, 1971.
[91] P. Hofmann, M.E. Markiewiecz, J.L. Spino, Nucl. Technol. 90 (1990) 226.
[92] F. Thevenot, M. Bouchacourt, L’Industrie Ceramique No. 732 (1979) 655.
[93] H. Kleykamp, G. Schumacher, Ber. Bunsenges. Phys. Chem. 97 (1993) 799.
[94] J. Drowart, G. de Maria, M.G. Inghram, J. Chem. Phys. 29 (1958) 1015.
[95] M. Rohde, J. Nucl. Mater. 182 (1991) 87.
[96] R.R. Dubin, Mater. Perform. 20 (1981) 13.
[97] H. Kleykamp, V. Schauer, A. Skokan, J. Nucl. Mater. 227 (1995) 130.
[98] M. Hillert, S. Jonsson, Z. Metallkd. 83 (1990) 720.
[99] P. McAllister Dryburgh, UK Pat. 2127709, 1984.
[100] H. Kotsch, G. Putzky, Abh. der Dt. Akad. der Wissensch. zu Berlin, Kl. f. Math. Phys. Techn. 1 (1966) 249.
[101] M. Billy, J. Mexmain, Sprechsaal 118 (1985) 245.
[102] G. Long, L.M. Foster, J. Am. Ceram. Soc. 42 (1959) 53.
[103] P. Boch, J.C. Glandus, J. Jarridge, J.P. Lecompte, J. Mexmain, Ceram. Int. 8 (1982) 34.
[104] R.D. Pehlke, J.F. Elliott, Trans. Met. Soc. AIME 215 (1959) 781.

[105] D.S. Neel, C.D. Pears, S. Oglesby, WADD-TR-60-924, 1962.
[106] M. Bennett, M.R. Houlton, J. Mater. Sci. 14 (1979) 184.
[107] O. Glemser, K. Beltz, P. Naumann, Z. Anorg. Allgem. Chem. 291 (1957) 51.
[108] R.N. Singh, J. Am. Ceram. Soc. 59 (1976) 112.
[109] R. Lowrie, NP-10401, 1961.
[110] G.V. Samsonov, High Temperature Compounds of Rare Earth Metals with Nonmetals, New York, 1965, p. 164.
[111] M.D. Lyutaya, A.B. Goncharuk, Redkozemel. Metal. Ikh Soedin. (1970) 128.
[112] H. Holleck, in: A.J. Freeman, C. Keller (Eds.), Handbook of the Physics and Chemistry of the Actinides, vol. 4, North-Holland, Amsterdam, 1986, p. 209.
[113] J.C. Hedge, J.W. Kopec, C. Kostenko, J.I. Lang, ASD-TDR-63-597, 1963.
[114] H. Holleck, F. Thümmler, Montsh. Chem. 98 (1967) 133.